First-Principles Theory of Quantum Well Resonance in Double Barrier Magnetic Tunnel Junctions

Yan Wang,[1] Zhong-Yi Lu,[2] X.-G. Zhang,[3,*,†] and X. F. Han[1,*,‡]

[1]*State Key Laboratory of Magnetism, Beijing National Laboratory for Condensed Matter Physics, Institute of Physics, Chinese Academy of Sciences, Beijing 100080, China*

[2]*Institute of Theoretical Physics, Chinese Academy of Sciences, Beijing 100080, China*

[3]*Center for Nanophase Materials Sciences and Computer Science and Mathematics Division, Oak Ridge National Laboratory, Oak Ridge, Tennessee 37831-6164, USA*

(Received 13 June 2006; published 25 August 2006)

Quantum well (QW) resonances in Fe(001)/MgO/Fe/MgO/Fe double barrier magnetic tunnel junctions are calculated from first principles. By including the Coulomb blockade energy due to the finite size islands of the middle Fe film, we confirm that the oscillatory differential resistance observed in a recent experiment [T. Nozaki *et al.*, Phys. Rev. Lett. **96**, 027208 (2006)] originates from the QW resonances from the Δ_1 band of the Fe majority-spin channel. The primary source of smearing at low temperatures is shown to be the variation of the Coulomb blockade energy.

DOI: 10.1103/PhysRevLett.97.087210 PACS numbers: 85.75.Mm, 72.25.Ba, 73.21.Fg, 73.23.Hk

The tunneling magnetoresistance (TMR) effect [1–3] in magnetic tunnel junctions (MTJs) has been the focus of spin-dependent transport studies in the past decade. Combining spin-dependent tunneling with resonant tunneling through quantum well (QW) states has also been studied using various layered structures [4–8]. Theoretical predictions of large boosts in the TMR due to QW resonances [7,8] attracted considerable interest in such studies. Earlier experiments [4,5] observed a very small effect that was attributed [8] partly to smearing from the amorphous barrier layers used in the studies. Recent success [9] in achieving a large TMR ratio of over 200% at room temperature in Fe/MgO/Fe(100) epitaxial single junctions raised the expectation of observing the QW resonance effect in the double junctions made of the same materials. Indeed, the new report of Nozaki *et al.* [6] showed oscillations in dI/dV as a function of the bias voltage. However, the effect is still too small to significantly affect the TMR.

A theoretical description for the QW resonance effect in a double barrier magnetic tunnel junction (DBMTJ) so far is limited to qualitative models [7]. The epitaxial systems based on Fe(100) electrodes and the MgO barrier layers, however, require an understanding based on first-principles calculation to distinguish between the effect of the multiple bands present at the Fermi energy in Fe and to correctly identify the QW states. Earlier first-principles work [10] in single barrier Fe/MgO/Fe junctions showed the importance of the Fe(100) Δ_1 band in producing nearly half-metallic spin polarization of the tunneling current. Because of the predominant s character of the Δ_1 band and its preferential transmission in the MgO barrier layer, this band is also the primary candidate for producing QW resonances [8]. Similar to single barrier MTJs, first-principles theory is also a critical step in understanding the QW resonances in double barrier junctions.

In this Letter we present a first-principles calculation of the QW states in the symmetric epitaxial Fe(001)/MgO/Fe/MgO/Fe DBMTJs. We demonstrate the existence of sharp spin-dependent Δ_1 QW states within the ultrathin middle Fe(001) film from the electronic structure calculation. By matching these QW states to the oscillations found in the experimental measurement [6], we confirm that these oscillations are indeed caused by the QW states at the $\bar{\Gamma}$ point with the Δ_1 symmetry in the middle Fe film. The shifts in the QW resonances due to the Coulomb blockade (CB) effect are used to estimate the size of the possibly discontinuous middle Fe film, whose scaling with the thickness is shown to be in good agreement with a previous atomic force microscopy (AFM) study [11]. We will also discuss the smearing effect of the CB on the QW resonances.

Similar to previous calculations [8,10], the electrode layers of bulk Fe and the middle Fe film are fixed at the lattice constant of 2.86 Å and the MgO lattice constant is taken to be a factor of $\sqrt{2}$ larger than that of the iron. This allows all of the layers to match epitaxially. The MgO barrier is fixed at four monolayers (ML), corresponding to a thickness of 1 nm. This is enough to provide a barrier for electron confinement in the middle metallic layer. The thickness of the middle Fe film is varied from 5 ML to 35 ML. All calculations are performed using the layer Korringa-Kohn-Rostoker (KKR) implementation [12] of the local spin density approximation of the density functional theory. The self-consistent calculation is performed in the same manner as in Refs. [8,10,13]. Once the electronic structure is converged, the $\mathbf{k}$-resolved density of states (DOS) is calculated at the $\bar{\Gamma}$ point of the two-dimensional Brillouin zone.

At the $\bar{\Gamma}$ point the Δ_1 band is primarily of s character (angular momentum $l = 0$). In Fig. 1(a), we show the

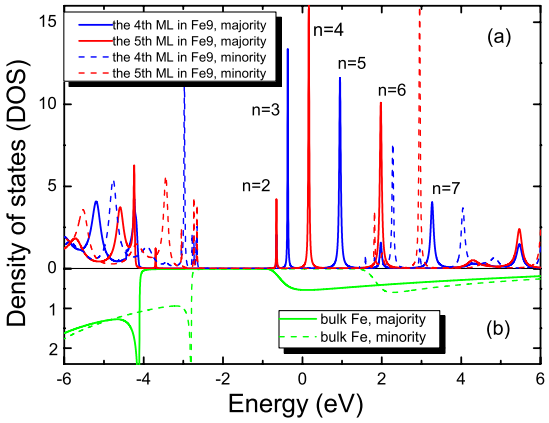

FIG. 1 (color online). s-resolved partial DOS at the $\bar{\Gamma}$ point. Solid line, majority spin; dashed line, minority spin. (a) Within the central Fe layer in bcc Fe(001)/MgO/Fe9/MgO/Fe. Red (gray) and blue (dark gray) lines represent the DOS for the middle atomic layer and one next to the middle layer in Fe9 film, respectively. (b) For bulk Fe. The Fermi energy is at 0 eV. n indicates the number of nodes in the wave function.

calculated s-resolved partial DOS at the $\bar{\Gamma}$ point within the central Fe layer in bcc Fe(001)/MgO/Fe9/MgO/Fe, with a 9 ML thickness of the Fe layer, compared with the s partial DOS in bulk Fe in Fig. 1(b). We assume that all of the Fe layer moments are aligned parallel in this system. The bottom of the conduction band in the MgO barrier is about 3.8 eV above the Fermi energy. In the majority channel the Δ_1 band of bulk Fe starts at about 0.9 eV below the Fermi energy. Within the energy range from -0.9 to 3.8 eV in Fig. 1(a) several sharp spikes in the DOS indicate the existence of majority-spin QW states derived from the Δ_1 band of the middle Fe film. The small coupling through the MgO barrier layers to the electrodes makes the width of these peaks finite. The exponential decay of the wave function, however, is fast in the barrier region, which sufficiently confines these states. The wave functions of the majority-spin QW states extend throughout all 9 ML of the middle Fe film. The states with $n = 0$ and $n = 1$ (n is the number of nodes in the wave function as discussed below) are not shown in Fig. 1(a) clearly, due to their greatly reduced heights near -0.9 V, at the edge of the Δ_1 band. The minority-spin QW states, derived from the Δ_1 band of the minority Fe, are about 1.5 eV above the Fermi energy. For the experimentally applied bias voltage of about 1 to 2 V, the minority-spin QW states are outside the transport energy window. This is consistent with the absence of oscillatory conductance for the antiparallel moment alignment in Ref. [6].

If the Fermi energy is fixed at that of bulk Fe in the electrodes without any bias, the positions of these QW states in DBMTJs can be determined by the middle film thickness alone. Figure 2(a) shows the majority-spin QW state energies relative to the Fermi energy between -1 and

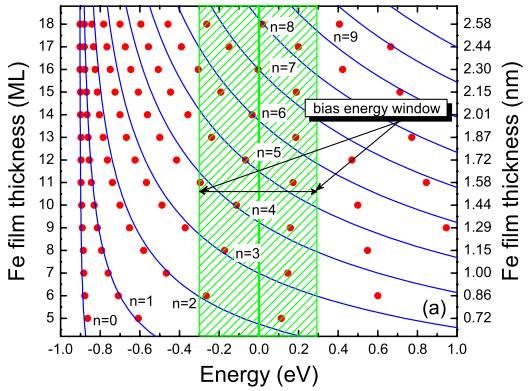

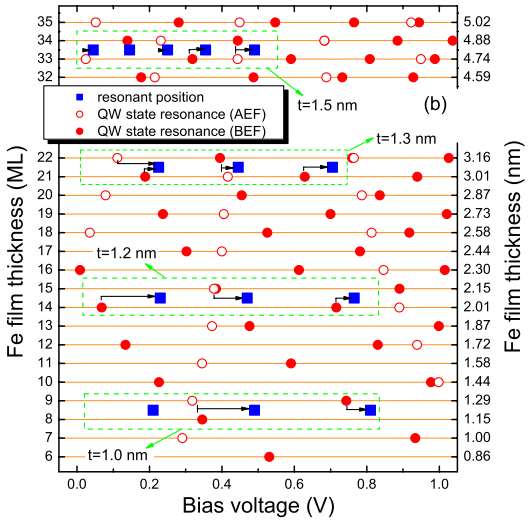

FIG. 2 (color online). (a) Majority-spin QW state energies relative to the Fermi energy in DBMTJs (denoted by circles). The lines are the PAM solutions. Shaded area represents the transport energy window in the middle Fe film when a bias voltage of 0.6 V is applied. (b) Applied bias voltage positions of the QW state resonances for different middle Fe film thickness. The circles are energies calculated from layer KKR. The squares are the resonant positions measured in Ref. [6]. Black arrows indicate the CB effect as discussed in the text.

1 eV for different middle Fe film thickness. These states can be classified according to the number n of nodes in the envelope electron wave functions. When a bias voltage is applied to a symmetric double barrier junction, the Fermi energy of one of the electrodes is shifted $V/2$ higher and the other $V/2$ lower than that of the middle Fe film. Thus the energy window for the middle Fe film is from $-V/2$ to $V/2$, as indicated by the shaded area in Fig. 2(a). Only QW states within this window contribute to the resonant tunneling. Both QW states above E_F (AEF) and below E_F (BEF) can contribute, and the order is determined by the absolute distance $|E - E_F|$ only. Note that the QW state with $n = 7$ for the thickness of 16 ML is very close to the Fermi energy. A very high TMR could be produced using a

very small bias voltage by setting the middle Fe film at about 2.3 nm.

We can compare the QW states obtained from the electronic structure calculation with the simple phase accumulation model (PAM), which is often used to describe the quantization condition of QW states [14,15], as shown in Fig. 2(a) as the solid lines. According to the PAM, the quantization condition for the existence of a QW state is given by

$$2k_\perp d - \Phi_1 - \Phi_2 - \Phi = 2\pi n, \quad (1)$$

where $k_\perp = \sqrt{2m^*(E - E_L)}/\hbar$ is the crystal momentum wave vector in the film perpendicular to the Fe/MgO interface, d is the Fe film thickness, and $\Phi_1 = \Phi_2 = 2\sin^{-1}\sqrt{(E - E_L)/(E_U - E_L)} - \pi$ is the phase shift on reflection at two Fe/MgO interface. Here m^* is the effective mass of majority-spin Fe, and E_L and E_U are the energies of the lower and upper edges of the band gap. We set $E_L = -0.9$ eV and $E_U = 3.8$ eV, and obtain $m^* \approx 4$ from the curvature of the Δ_1 band. Φ is the additional phase shift to account for interface roughness. The best fit near the Fermi energy to the first-principles result is obtained for the PAM if we use $\Phi = 0.6\pi$. From Fig. 2(a) it is clear that the first-principles calculation and the PAM agree well for the low n QW states, but large errors develop in the PAM solutions with $n > 3$. We conclude that the PAM offers only a qualitative description of the QW states.

In Fig. 2(b), the calculated QW state resonances for different middle Fe film thickness are compared with the experimental resonant voltages [6] (denoted by squares), for four different nominal thicknesses, $t = 1.0$, 1.2, 1.3, and 1.5 nm, respectively. A resonance voltage of the experimental data is taken to be the midpoint between a local maximum and its next minimum on the dI/dV-V curve, corresponding approximately to the maximum of the tunneling current as a function of voltage. The four sets of data are matched to the theoretical QW resonances if the actual thicknesses of the middle Fe film are taken to be 1.2 nm (8–9 ML), 2 nm (14–15 ML), 3 nm (21–22 ML), and 4.8 nm (33–34 ML) [16], respectively. The Fe films may consist of small regions of varying thicknesses, so the data are averaged over two nearby layers, as shown in Fig. 2(b) within the dashed boxes for each case. The first peak in conductance curve for the $t = 1.0$ nm sample in Ref. [6] yields a possible resonance at about 0.21 V. No Δ_1 QW state can be found to correspond to this resonance. It is likely a resonance from another **k** point or is unrelated to QW states.

There is a consistent positive voltage difference between the calculated resonances and the corresponding observed ones. This is due to the Coulomb charging energy in the middle Fe film. In the experiment the actual middle Fe film is likely discontinuous. This leads to a finite Coulomb blockade energy that can be evaluated using a simple capacitance model. When an electron tunnels through the MgO barrier and onto the Fe island, the electrostatic energy E_c increases by $E_c = e^2/C_{\text{Fe-MgO}}$, where $C_{\text{Fe-MgO}}$ is the capacitance of the Fe-MgO junction. This presents an additional barrier of height E_c. The capacitance of the junction depends on the thickness d_{MgO} of the MgO barrier and the area A of the Fe island. It can be approximated by that of a plate capacitor $C_{\text{Fe-MgO}} = \varepsilon_0\varepsilon_{\text{MgO}}A/d_{\text{MgO}}$, where ε_0 is the electrical permittivity constant and ε_{MgO} is the dielectric constant of MgO. The total capacitance of a double junction is half of that of a single junction. Thus, the total capacitance of MgO/Fe-island/MgO is given by $C = C_{\text{Fe-MgO}}/2$. The CB voltage V_{CB} in DBMTJs can be express as $V_{\text{CB}} = E_c/e = e/C = 2e/C_{\text{Fe-MgO}} = \frac{2ed_{\text{MgO}}}{\varepsilon_0\varepsilon_{\text{MgO}}A}$.

The CB voltage V_{CB} as a function of island diameter is shown in Fig. 3(a) with the experimental values for $\varepsilon_{\text{MgO}} = 9.6$ [17] and $d_{\text{MgO}} = 2$ nm. The Fe islands are assumed to be circular so that $A = \pi D^2/4$. Because of the different charge distribution of different QW states, in principle V_{CB} also varies with the QW states. For simplicity we average over all QW resonances for the same Fe film thickness to obtain an estimate of V_{CB} independent of the QW states. We find $V_{CB} = 0.13$, 0.10, 0.06, and 0.03 V for the four nominal thicknesses $t = 1.0$, 1.2, 1.3, and 1.5 nm, respectively. From these values we estimate the diameters of the Fe island for each case as 8.5, 10, 12.5, and 17.5 nm, respectively. These values are plotted in Fig. 3(b). An earlier AFM analysis of granular Fe(110) thin films [11] found a similar relationship between the average island diameter and height (actual film thickness), as shown in Fig. 3(b). The open squares in Fig. 3(b) represent calculation using $d_{\text{MgO}} = 2.8$ nm. TEM pictures [18] show the MgO thickness of these samples to be 2 nm. The apparently larger effective capacitive thickness of the MgO film is probably due to the smaller dielectric constant of a thin film than that of the bulk insulator. In addition, the observed middle Fe film thickness is 5.3 nm [16] for the $t = 1.5$ nm sample, compared to 4.8 nm from matching the

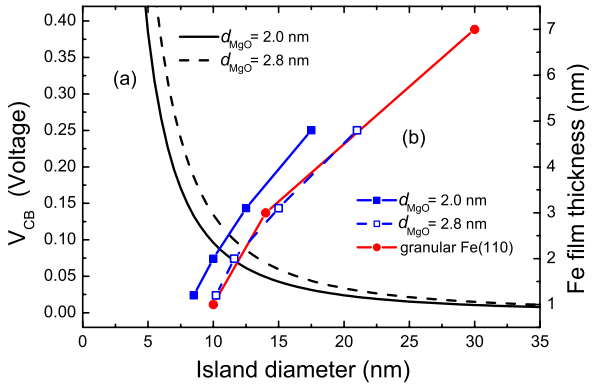

FIG. 3 (color online). (a) Island diameter dependence of the Coulomb charging energy V_{CB} in DBMTJs. (b) Variation of Fe film thickness versus estimated diameters of the Fe island (squares) in comparison with the cited similar results from Ref. [11] (circles).

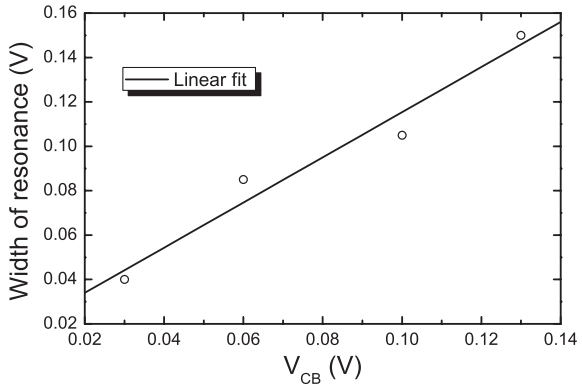

FIG. 4. Width of QW resonance as a function of the Coulomb charging energy V_{CB}. The linear fit is $y = x + 0.013$.

QW states. There is about 0.5 nm thickness of the middle layer that does not conduct. This could be either FeO or an interfacial roughness region which adding to the MgO layer leads to an effective capacitance thickness of about 2.5 nm. The formation of a partially oxidized FeO layer at the Fe/MgO interface [19] is also a possible reason that the resonances were observed only in the positive bias direction [6].

The wide distribution of the island size can lead to large differences in V_{CB} between separate islands. This factor adds to the smearing effect on the oscillatory QW resonances in the I-V curves. Although the smearing effect due to V_{CB} cannot be easily separated from that of diffuse scattering, a qualitative picture can be obtained by an analysis of the low temperature data. In Fig. 4 we show the width of the sharpest resonance in each dI/dV curve as a function of the estimated Coulomb charging energy V_{CB} for the same sample. The strong linear correlation between the two quantities is evident. Because the fluctuation in V_{CB} is approximately proportional to V_{CB}, this figure presents strong evidence that the smearing of the QW resonances is likely dominated by the CB effect at low temperatures.

In summary, we matched experimentally measured oscillatory I-V characteristics in Fe(001)/MgO/Fe/MgO/Fe DBMTJs to first-principles QW states at the $\bar{\Gamma}$ point of the majority-spin channel in the middle Fe film. The Coulomb blockade effect is shown to play an important role in these systems, determining both the position of a resonance as well as its sharpness. Our result points to a hopeful path for exploiting spin-dependent QW resonances that have so far eluded physicists. The key for reducing the smearing effect appears to be minimizing the CB energy. Thus fabricating a continuous and smooth middle Fe film is critical in such experiments.

The authors thank Dr. Nozaki for helpful discussions. This research was supported by the State Key Project of Fundamental Research of Ministry of Science and Technology (MOST) Grant No. 2001CB610601 and the Knowledge Innovation Program project of Chinese Academy of Science. X. F. H. gratefully acknowledges the partial support of the Outstanding Young Researcher Foundation (Grants No. 50325104 and No. 50528101), Chinese National Natural Science Foundation (NSFC, Grant No. 10574156), and the China-Ireland Research Collaboration Fund from both NSFC and MOST. X.-G. Z. thanks the Center for Nanophase Materials Sciences, which is sponsored at Oak Ridge National Laboratory by the Division of Scientific User Facilities, U.S. Department of Energy, for support.

*Corresponding author.
†Electronic address: xgz@ornl.gov
‡Electronic address: xfhan@aphy.iphy.ac.cn

[1] M. Julliere, Phys. Lett. **54A**, 225 (1975).
[2] T. Miyazaki and N. Tezuka, J. Magn. Magn. Mater. **139**, L231 (1995).
[3] J. S. Moodera, L. R. Kinder, T. M. Wong, and R. Meservey, Phys. Rev. Lett. **74**, 3273 (1995).
[4] S. Yuasa, T. Nagahama, and Y. Suzuki, Science **297**, 234 (2002).
[5] T. Nagahama, S. Yuasa, Y. Suzuki, and E. Tamura, J. Appl. Phys. **91**, 7035 (2002).
[6] T. Nozaki, N. Tezuka, and K. Inomata, Phys. Rev. Lett. **96**, 027208 (2006).
[7] X. Zhang, B.-Z. Li, G. Sun, and F.-C. Pu, Phys. Rev. B **56**, 5484 (1997).
[8] Zhong-Yi Lu, X.-G. Zhang, and Sokrates T. Pantelides, Phys. Rev. Lett. **94**, 207210 (2005).
[9] S. Yuasa, T. Nagahama, A. Fukushima, Y. Suzuki, and K. Ando, Nat. Mater. **3**, 868 (2004).
[10] W. H. Butler, X.-G. Zhang, T. C. Schulthess, and J. M. MacLaren, Phys. Rev. B **63**, 054416 (2001).
[11] E. Navarro, Y. Huttel, C. Clavero, A. Cebollada, and G. Armelles, Phys. Rev. B **69**, 224419 (2004).
[12] J. M. MacLaren, X.-G. Zhang, W. H. Butler, and Xindong Wang, Phys. Rev. B **59**, 5470 (1999).
[13] X.-G. Zhang, W. H. Butler, and Amrit Bandyopadhyay, Phys. Rev. B **68**, 092402 (2003).
[14] P. M. Echenique and J. B. Pendry, Prog. Surf. Sci. **32**, 111 (1989).
[15] N. V. Smith, N. B. Brookes, Y. Chang, and P. D. Johnson, Phys. Rev. B **49**, 332 (1994).
[16] Actual middle Fe film thickness was estimated to be 5.3 nm (2 nm) for $t = 1.5$ nm ($t = 1.2$ nm) from the cross-sectional TEM analysis in Ref. [6].
[17] *CRC Handbook of Chemistry and Physics*, edited by D. R. Lide (CRC Press, Boca Raton, FL, 2001), 82nd ed.
[18] Takayuki Nozaki (private communication).
[19] H. L. Meyerheim, R. Popescu, J. Kirschner, N. Jedrecy, M. Sauvage-Simkin, B. Heinrich, and R. Pinchaux, Phys. Rev. Lett. **87**, 076102 (2001).